



OPEN CD206 and dust particles are prognostic biomarkers of progressive fibrosing interstitial lung disease associated with air pollutant exposure

Aliaksei Kadushkin^{1,5}✉, Olga Yudina^{1,2}, Nastassia Lukashevich¹, Elena Davidovskaya^{1,3}, Vasyil Filanyuk¹, Volha Dziadzichkina¹ & Xiaoming Cai⁴

Current management strategies for progressive fibrosing interstitial lung disease (PF-ILD) and non-PF-ILD differ significantly, underscoring the need for early identification of PF-ILD patients. We analyzed the expression of macrophage markers and the number of dust particles (DP) in lung tissue, as well as complete blood count and blood chemistry tests to identify biomarkers of PF-ILD, and examined the effect of certain pollutants on these biomarkers. Lung biopsies were collected from 73 non-PF-ILD patients and 36 PF-ILD patients. DP were quantified in alveolar wall cells (DP-aw) and desquamated epithelial cells (DP-desq) using polarizing light microscopy. Expression of CD206, transforming growth factor β 1 (TGF- β 1), connective tissue growth factor (CTGF), C-X-C motif ligand 13 (CXCL13), fibroblast growth factor 2 (FGF-2), tumor necrosis factor α (TNF α), and interleukin 1 β (IL-1 β) was assessed in lung tissue by immunohistochemistry. The numbers of DP-desq, pulmonary expression of CXCL13, IL-1 β and CD206 were higher in ILD patients resided for ≥ 15 days per year in places with 24-hour ambient PM₁₀ level of $\geq 50 \mu\text{g}/\text{m}^3$ compared with ILD patients exposed for < 15 days per year to the similar PM₁₀ concentration. Additionally, CXCL13 expression in lung tissue was higher in smoking ILD patients than in non-smoking ILD patients. Compared with non-PF-ILD patients, PF-ILD patients exhibited higher numbers of DP-aw and DP-desq, as well as increased expression of CD206, CXCL13, IL-1 β , TGF- β 1, and CTGF in lung tissue. Elevated blood neutrophil-to-lymphocyte (NLR) and platelet-to-lymphocyte ratios were also observed in PF-ILD patients. These biomarkers were found to be independent predictors of PF-ILD. A regression logistic model incorporating NLR, CD206, and DP-desq predicted PF-ILD with an AUC of 0.847, sensitivity of 84.6%, and specificity of 83.3%. Our findings may be useful in predicting PF-ILD and highlight the need for reducing pollutant emission.

Keywords CD206, CXCL13, Progressive fibrosing interstitial lung disease, PM₁₀ concentration, Biomarkers, Dust particles

Abbreviations

AISI	Aggregate index of systemic inflammation
AUC	Area under the ROC curve
CRP	C-reactive protein
CTGF	Connective tissue growth factor
CXCL13	C-X-C motif ligand 13
DL _{CO}	Diffusing capacity of the lung for carbon monoxide
DP	Dust particles
DP-aw	Dust particles in the alveolar wall cells

¹Belarusian State Medical University, Minsk 220083, Belarus. ²Republican Clinical Medical Center of Administration of the President of the Republic of Belarus, Zhdanovichy Rural Council, Minsk District 223028, Belarus. ³Republican Scientific and Practical Center of Pulmonology and Phthisiology, Minsk 220080, Belarus. ⁴School of Public Health, Soochow University, Suzhou 215123, Jiangsu, China. ⁵Department of Biological Chemistry, Belarusian State Medical University, Minsk, Belarus. ✉email: kadushkyn@gmail.com

DP-desq	Dust particles in the desquamated epithelial cells
FGF-2	Fibroblast growth factor 2
FVC	Forced vital capacity
HRCT	High-resolution computed tomography
IHC	Immunohistochemistry
IL	Interleukin
ILD	Interstitial lung disease
IPF	Idiopathic pulmonary fibrosis
LMR	Lymphocyte-to-monocyte ratio
NLR	Neutrophil-to-lymphocyte ratio
PFT	Pulmonary function tests
PF-ILD	Progressive fibrosing interstitial lung disease
PLR	Platelet-to-lymphocyte ratio
PM _{2.5}	Particulate matter $\leq 2.5 \mu\text{m}$ in diameter
PM ₁₀	Particulate matter $\leq 10 \mu\text{m}$ in diameter
SIRI	Systemic inflammatory response index
TGF- β 1	Transforming growth factor β 1
TNF α	Tumor necrosis factor α
VATS	Video-assisted thoracoscopic surgery

Idiopathic pulmonary fibrosis (IPF) is a chronic, progressive fibrosing interstitial lung disease (ILD) of unknown etiology, which is characterized by high mortality¹. The median survival age for patients with IPF without treatment is estimated at 3–5 years². Even with adequate management, pulmonary fibrosis can also progress within 6–24 months in 31–48% of patients with other forms of ILD³, in particular, chronic hypersensitivity pneumonitis, idiopathic non-specific interstitial pneumonia, connective tissue disease-associated ILD, unclassifiable ILD, occupational ILD, sarcoidosis, and others⁴. Patients with other than IPF forms of ILD with a progressive fibrosing phenotype (PF-ILD) have a shorter life expectancy than patients with ILD without a progressive phenotype (non-PF-ILD). Moreover, the clinical course (without proper therapy) and unfavorable prognosis for mortality are similar in patients with PF-ILD and IPF^{5,6}.

Current management strategies for PF-ILD and non-PF-ILD differ significantly, underscoring the need for timely identification of patients with PF-ILD. Early diagnosis is crucial for the effectiveness in slowing lung function decline, safety and tolerability of antifibrotic therapy (nintedanib and pirfenidone) in patients with PF-ILD⁷. In addition, lung transplantation should be considered in patients with advanced PF-ILD⁸. However, there are still no reliable, validated biomarkers that could be used to predict the progression of pulmonary fibrosis in patients with non-IPF forms of ILD^{7,9}.

Air pollutants, including particulate matter (PM) $\leq 10 \mu\text{m}$ in diameter (PM₁₀), PM $\leq 2.5 \mu\text{m}$ in diameter (PM_{2.5}), nitrogen dioxide (NO₂), other nitrogen oxides (NO_x), carbon monoxide (CO) and ozone (O₃), through several molecular mechanisms may affect the risk of IPF incidence and health outcomes such as disease severity and progression, risk of acute exacerbation, hospitalization and mortality^{10,11}. However, no tight association of ambient pollutant exposure with the progression of non-IPF fibrosing ILDs has been established. Inorganic dust particles (DP) such as PM₁₀ and PM_{2.5} can be deposited in large and small airways of patients with ILDs¹². Previous studies have detected DP in lung tissue samples of patients with IPF and non-IPF ILDs^{13–16}. These DP cause mucociliary dysfunction, induce epithelial permeability, and epithelial-mesenchymal transition (EMT)^{11,17,18}. Moreover, inhalation of air pollution particles leads to the activation of macrophages, which subsequently produce proinflammatory and profibrogenic mediators (cytokines, chemokines, enzymes)¹⁹.

Depending on the microenvironment, macrophages can polarize into M1 and M2 subtypes (M2a, M2b, M2c, and M2d)²⁰. Classically activated M1 macrophages drive proinflammatory responses and produce interleukin 1 β (IL-1 β), IL-6, IL-8, IL-12, IL-23, tumor necrosis factor α (TNF α), C-X-C motif ligand 9 (CXCL9), CXCL10, CXCL11. Alternatively activated M2 macrophages promote anti-inflammatory responses and stimulate profibrotic processes such as EMT. M2 macrophage subtype has been shown to express IL-1 β , IL-10, transforming growth factor β 1 (TGF- β 1), connective tissue growth factor (CTGF), fibroblast growth factor 2 (FGF-2), CXCL13, TNF α , and mannose receptor C type 1 (MRC1, CD206)^{20,21}.

In this study, we hypothesized that the detection of DP and macrophage markers in the lungs of non-IPF-ILD patients exposed to environmental pollutants could be used to predict progressive fibrosis. We determined DP in the alveolar wall and desquamated epithelial cells, along with intracellular (TGF- β 1, CTGF, CXCL13, FGF-2) and cell-surface (CD206) markers of M2 macrophages, cytokines produced by both M1 and M2 macrophages (TNF α , IL-1 β) in lung tissue of PF-ILD and non-PF-ILD patients. Additionally, in these groups of patients we assessed the prognostic ability of complete blood count and blood chemistry tests, which were recently found to predict mortality and clinical risk in IPF^{22–24}. Finally, we examined the effect of certain pollutants (PM₁₀, CO, NO₂, NO_x, SO₂, ammonia, and ground-level O₃) on DP accumulation and macrophage marker expression in lung tissue of ILD patients.

Methods

Patients

This observational retrospective cohort study was performed at the Republican Scientific and Practical Center of Pulmonology and Phthisiology, Minsk, Belarus. We retrospectively screened all patients aged ≥ 18 years with a confirmed diagnosis of fibrosing ILDs other than IPF who underwent video-assisted thoracoscopic surgery (VATS) procedure between January 1, 2015 and December 31, 2021. Multidisciplinary diagnostics of ILDs were carried out by a pulmonologist, radiologist, rheumatologist, and pathologist based on clinical characteristics,

high-resolution computed tomography (HRCT), and surgical lung biopsy. Patients with available results of pulmonary function tests (PFT) and HRCT as well as the severity of respiratory symptoms at baseline and within 2 years of follow-up were enrolled in the study. Following were the exclusion criteria: (1) fibrotic extent < 10% on baseline HRCT, (2) first follow-up PFT and HRCT were performed > 24 months after baseline PFT and HRCT, (3) diagnosis of pulmonary embolism, decompensated heart failure, or lower respiratory tract infections associated with disease progression, (4) lung cancer at baseline, and (5) occupational ILD (Fig. 1).

Data collection

We reviewed inpatient and outpatient medical records to extract data at the first clinical visit and within ≥ 2 years, including demographic information, physical examination, HRCT images, and PFT results. Blood and lung biopsy samples were collected from patients, who did not have an acute exacerbation of ILD, at the first hospital admission (before potential fibrosis progression). A complete blood count was performed using a Cell-Dyn Ruby Hematology Analyzer (Abbott Laboratories, USA), blood chemistry tests were measured using an Architect c4000 Clinical Chemistry Analyzer (Abbott Laboratories, USA), and haemostasis parameters were processed using a Helena AC-4 automated coagulometer (Helena Biosciences, UK).

PF-ILD assessment

PF-ILD was defined (according to the INBUILD trial) in patients who fulfilled ≥ 1 of the following criteria within the 24 months of follow-up, despite clinically appropriate management: (1) a relative decline in the forced vital

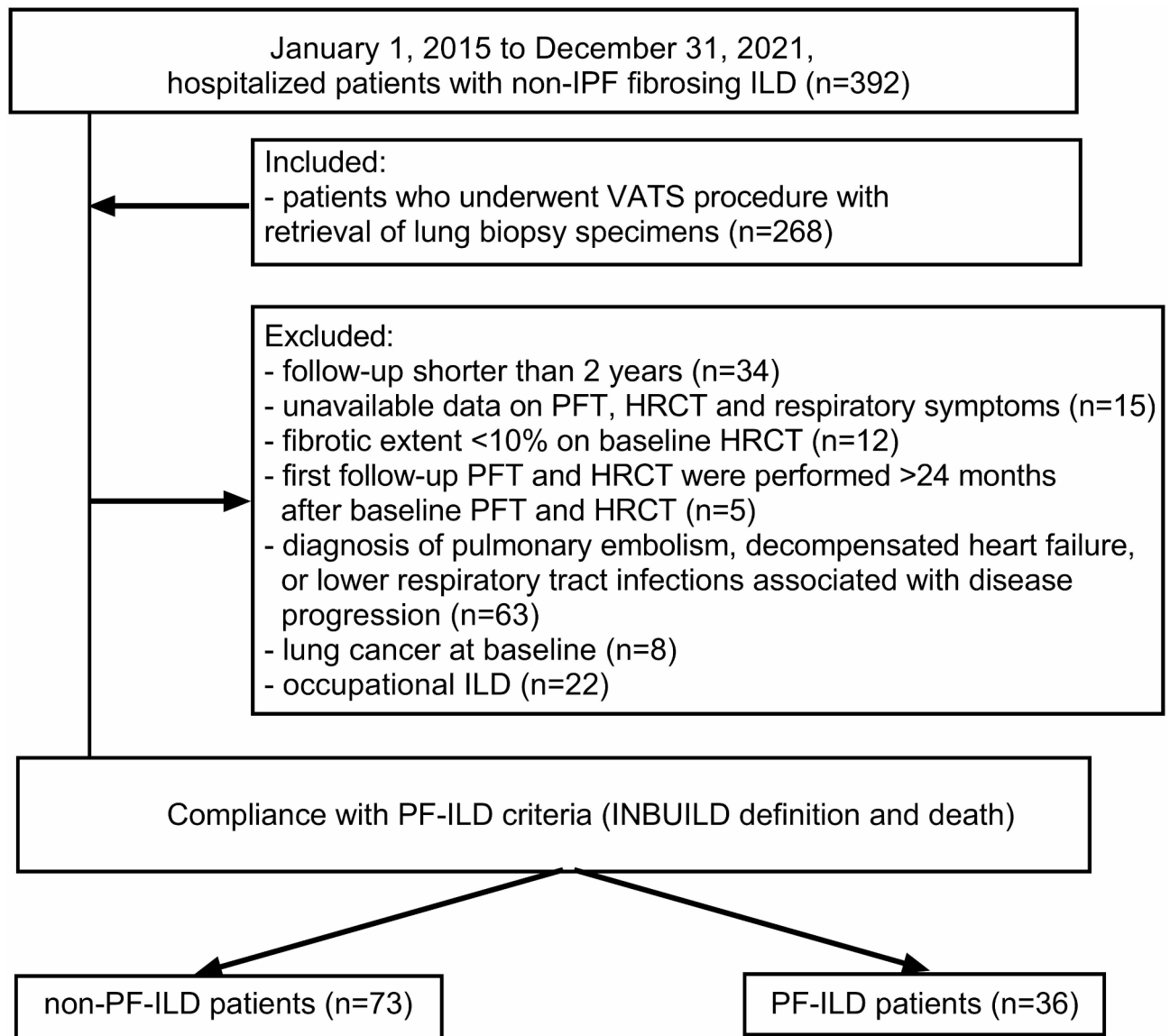


Fig. 1. Study flow chart. *HRCT* high-resolution computed tomography, *ILD* interstitial lung disease, *IPF* idiopathic pulmonary fibrosis, *PF-ILD* progressive fibrosing interstitial lung disease, *PFT* pulmonary function tests, *VATS* video-assisted thoracoscopic surgery.

capacity (FVC) $\geq 10\%$ of the predicted value; (2) a relative decline in the FVC $\geq 5\%$ to $< 10\%$ of the predicted value and an increased extent of fibrosis on HRCT or worsened respiratory symptoms; (3) increased extent of fibrosis on HRCT and worsened respiratory symptoms²⁵. In addition, patients who died of any cause within 2 years of follow-up were also considered to have PF-ILD²⁶.

Reagents and materials

Rabbit polyclonal antibodies to TNF α (catalogue No. ab6671) and CTGF (catalogue No. ab5097), as well as rabbit monoclonal antibody to FGF-2 (catalogue No. ab92337) were from Abcam (Cambridge, UK). Rabbit polyclonal antibodies to IL-1 β (catalogue No. PAA563Hu06), TGF- β 1 (catalogue No. PAA124Hu01), and CXCL13 (catalogue No. PAB601Hu01) were purchased from Cloud Clone Corp. (Wuhan, China). Rabbit polyclonal antibody against CD206 (catalogue No. abx177447) was obtained from Abnova Ltd. (Cambridge, UK). Sodium Citrate Antigen Retrieval Solution (catalogue No. E-IR-R105) was from Elabscience (Wuhan, China), and eBioscience IHC Antigen Retrieval Solution (catalogue No. 00-4956-58) was obtained from Invitrogen (Thermo Fisher Scientific, Inc., Waltham, MA, USA). Antibody Diluent (catalogue No. ZD19), Tris Buffered Saline Wash Buffer (TBS Wash Buffer, catalogue No. ZD4) and Universal HRP Polymer Detection Kit (catalogue No. ZD11) consisting of anti-mouse horseradish peroxidase (HRP)/anti-rabbit HRP, 3,3'-diaminobenzidine (DAB) Chromogen Concentrate, and DAB Substrate buffer, were purchased from Zeta Corporation (Arcadia, CA, USA). Eprelia Cytoseal 60 mounting media (catalogue No. 23-244257) was from Thermo Fisher Scientific. Hydrogen Peroxide Blocking Reagent (catalogue No. ACA125) was from ScyTec Laboratories (West Logan, UT, USA).

Assessment of lung fibrosis

To evaluate the histological features of pulmonary fibrosis, lung tissue sections were stained using the Masson's trichrome kit²⁷. The extent of fibrosis was independently examined by two pathologists (O. Y. and N. L.) in at least 10 randomly selected fields for each sample using Positive Pixel Count algorithm embedded in the Aperio ImageScope software (version 12.4.3.5008, Leica Biosystems Imaging, Inc., Vista, CA, USA). To quantify the percentage of tissue with fibrotic changes (fibrosis score), the pixel count for fibrotic tissue area was divided by the pixel count for total lung tissue area, and multiplied by 100.

Analysis of dust particles in lung tissue

To count the DP, Masson's trichrome stained slides were screened using a Leica DM2500 optical microscope (Leica Microsystems Inc., Deerfield, IL, USA) under polarizing light with 200 \times magnification (objective ~ 0.17 /OFN25 HI PLAN 20 \times /0.40), and if necessary, 400 \times magnification (objective ~ 0.17 /OFN25 HI PLAN 40 \times /0.65). The numbers of the birefringent DP in 10 random fields of view were measured in the alveolar wall cells (DP-aw) and in the desquamated epithelial cells (DP-desq).

Immunohistochemical analysis

Immunohistochemistry (IHC) was performed as previously described^{28,29}. Briefly, 4 μ m thick formalin-fixed paraffin-embedded lung tissue sections were deparaffinized (using xylols) and rehydrated (using graded ethanol solutions and distilled water). Heat-mediated antigen retrieval was performed by immersing slides in 1X eBioscience IHC Antigen Retrieval Solution at pH 9.0 (or 1X Sodium Citrate Antigen Retrieval Solution at pH 6.0, for detection of TGF- β 1) at 125 $^{\circ}$ C in a DakoCytomation Pascal S2800 pressure chamber (Dako, Carpinteria, CA, USA). Endogenous peroxidase activity was inhibited by incubation of slides with ScyTec Peroxide Block for 10 min at room temperature. Nonspecific binding of antibodies to the tissues was reduced by the pretreatment of sections with 1.0% bovine serum albumin in TBS Wash Buffer for 30 min at room temperature. Sections were next incubated with primary rabbit antibodies to IL-1 β (1:200 dilution), TGF- β 1 (1:150 dilution), CXCL13 (1:1000 dilution), TNF α (1:125 dilution), CTGF (1:250 dilution), FGF-2 (1:2400 dilution), and CD206 (1:100 dilution), or an IgG control antibody. To dilute all antibodies, Zeta Antibody Diluent was applied. Slides were washed twice using TBS Wash Buffer (5 min each), and the sections were treated with polymer HRP-conjugated anti-mouse/anti-rabbit IgG secondary antibodies (without dilution) for 30 min at room temperature. The slides were washed twice using TBS Wash Buffer (5 min each). Immunostaining was visualized using the mixture (1:20) of DAB Chromogen Concentrate and DAB Substrate buffer. The sections were counterstained with Mayer's hematoxylin (2 min at room temperature) for detection of membrane (CD206) and cytoplasmic (all other) proteins. The sections were dehydrated and mounted with Eprelia Cytoseal 60 mounting media.

High-resolution digital images (0.26 μ m/pixel) were generated using a Motic ScanEasy Pro 6 scanner system (Motic, Kowloon, Hong Kong). Quantitative analysis of biomarker expression was performed using the Aperio ImageScope software (version 12.4.3.5008) as previously reported^{28,29}. The positivity of expression (percentage of positive pixels in the analyzed area) was evaluated as the number of positive pixels divided by the total number of pixels (positive and negative), and multiplied by 100. The corresponding intervals that allowed pixel intensity to be classified as positive and negative were 0–220 and 220–255, respectively. All measurements of digital images were repeated at least three times by two independent pathologists (the second and third authors), and the mean values were evaluated.

Impact of air pollution on the biomarker expression in lung tissue of patients with ILD

The level of air pollution at the residential areas of patients with ILD was assessed based on the data provided by the Republican center for hydrometeorology, control of radioactive contamination and environmental monitoring (Minsk, Belarus). In particular, we analyzed annual mean levels of pollutants (PM₁₀, NO₂, NO_x, CO, SO₂, ammonia, ground-level O₃) collected at the air quality monitoring stations nearest to the patients' home addresses (< 3.5 km from the subjects' place of living), as well as the number of days with exceedance of

the Belarus air quality guideline (BAQG) level for daily average of these pollutants. The association between the number of DP in the lungs of patients with ILD, as well as the pulmonary expression of biomarkers and the air pollutant concentrations at the patients' homes was determined.

Statistical analysis

Results are reported as median and interquartile range (IQR). Variable distribution was evaluated by the Shapiro-Wilk test. Comparisons between two groups were carried out using the Mann-Whitney *U* test and the χ^2 test. Spearman correlation was applied to detect associations between biomarker expression and clinical parameters or air pollution exposure. Logistic regression analysis was performed to assess the efficacy of M1/M2 macrophage markers, DP and blood tests as predictors of PF-ILD. Receiver operating characteristic (ROC) curve was created to estimate the area under the curve (AUC). The optimal cut-off values for predictors were determined according to the Youden index. For all tests, *p* values of < 0.05 were considered statistically significant. All calculations were performed using GraphPad Prism version 10.2.2.397 (GraphPad Software, San Diego, CA, USA) and MedCalc version 22.032 (MedCalc Software Ltd, Ostend, Belgium).

Results

Patients

The final cohort consisted of 109 patients with non-IPF-ILDs, of whom 36 subjects had a progressive fibrosing phenotype. In particular, within the 24 months of follow-up, 15 (41.7%), 13 (36.1%) and 3 (8.3%) patients met the criteria 1, 2, 3 for PF-ILD, respectively. In addition, 5 patients (13.9%) who died within 2 years were classified into the PF-ILD group. The most frequent diagnoses of ILDs among all patients were non-IPF idiopathic non-specific interstitial pneumonia (36 patients, 33.0%), unclassifiable ILD (34 patients, 31.2%), connective tissue disease-associated ILD (25 patients, 22.9%), chronic hypersensitivity pneumonitis (10 patients, 9.2%), and sarcoidosis (4 patients, 3.7%). None of the patients used antifibrotic treatment (nintedanib or pirfenidone) at baseline or during 2 years of follow-up. Patient characteristics are described in the Table 1.

Dust particles in lung tissue samples of patients with ILD

Birefringent DP were found in lung tissue samples from all patients with non-IPF-ILDs. The absolute number of DP observed in 10 random fields of view ranged from 4 to 1085 per sample. The amount of DP-aw in the cells of thickened alveolar wall was higher in patients with PF-ILD than in patients with non-PF-ILD (Fig. 2). DP-desq were also more frequently presented in the desquamated epithelial cells within the alveolar spaces of patients with PF-ILD compared with non-PF-ILD patients.

Biomarker expression in lung tissue specimens

The expression of macrophage markers in lung tissue samples from patients with non-IPF ILDs was assessed by IHC. Image analysis using the percentage of positive pixels revealed significantly increased CXCL13 and CD206 expression in the lungs of PF-ILD patients compared with specimens from non-PF-ILD patients (Fig. 3). The levels of IL-1 β , TGF- β 1 and CTGF were also higher in lung tissue of PF-ILD patients compared with non-PF-ILD patients (Figs. 3 and 4). However, quantitative image analysis of TNF α and FGF-2 expression showed no significant difference between PF-ILD and non-PF-ILD patients. Moreover, a similar fibrosis score was observed in patients with PF-ILD and non-PF-ILD (Fig. 4).

Intrapulmonary expression of CXCL13, IL-1 β , and CD206 was higher in patients with ≥ 50 DP-desq in lung tissue (calculated in 10 random fields of view per sample) than in patients with < 50 DP-desq (Supplementary Fig. 1). In addition, the number of DP-desq was positively correlated with the expression levels of CXCL13 ($R=0.275$, $p=0.004$), IL-1 β ($R=0.285$, $p=0.003$), and CD206 ($R=0.258$, $p=0.007$) in lung tissue from ILD patients.

Complete blood count tests and blood chemistry tests in patients with ILDs

The neutrophil-to-lymphocyte ratio (NLR), platelet-to-lymphocyte ratio (PLR), systemic inflammatory response index (SIRI), and aggregate index of systemic inflammation (AISI) were substantially increased in the PF-ILD group compared with non-PF-ILD patients (Table 1). Additionally, peripheral blood concentrations of C-reactive protein (CRP), fibrinogen and D-dimer were higher in PF-ILD patients than in non-PF-ILD subjects. However, incomplete data on blood chemistry tests and haemostasis parameters in patients with ILDs limited the inclusion of CRP, fibrinogen and D-dimer in subsequent logistic regression analysis.

Association of biomarker expression and air pollution exposure

In total, 97 patients with ILDs were included into the analysis aimed at finding associations between air pollution exposure and biomarker expression. Unfortunately, 12 patients were excluded from this part of study due to the lack of air monitoring stations located within 3.5 km of their homes. Among the remaining patients, those ($n=57$) living in areas with daily average PM₁₀ concentrations exceeding the BAQG level ($> 50 \mu\text{g}/\text{m}^3$) for ≥ 15 days showed higher numbers of DP-desq and increased pulmonary expression of CXCL13, IL-1 β , and CD206 compared with patients ($n=40$) exposed to PM₁₀ concentrations below this threshold for < 15 days (Fig. 5). The annual mean level of PM₁₀ at the patient's place of residence was weakly correlated with the number of DP-desq ($R=0.314$, $p=0.002$) and CXCL13 expression ($R=0.227$, $p=0.026$) in the lungs of ILD patients. Moreover, we revealed a significant association between mean annual concentration of NO₂ and expression of CXCL13 ($R=0.322$, $p=0.001$), CD206 ($R=0.224$, $p=0.028$), and IL-1 β ($R=0.322$, $p=0.001$) in lung tissue of patients with ILD. The number of DP and positivity of pulmonary biomarker expression were not associated with annual mean concentrations of CO, NO_x, SO₂, ammonia, and ground-level O₃ in the ambient air. Among complete

Characteristic	All	Non-PF-ILD patients	PF-ILD patients	p-value
Number	109	73	36	
Age, years	62.0 (56.0–67.0)	62.0 (55.8–66.0)	62.5 (57.0–69.5)	0.280
Male, n (%)	74 (67.9%)	49 (67.1%)	25 (69.4%)	0.808
BMI, kg/m ²	25.0 (23.0–29.0)	25.0 (23.0–29.3)	25.0 (22.5–27.0)	0.235
^a Former or current smoker, n (%)	57 (52.3%)	38 (52.1%)	19 (52.8%)	0.944
Pulmonary function tests				
FVC, % predicted	78.0 (66.0–87.0)	80.0 (69.8–87.0)	77.0 (64.5–83.0)	0.150
FEV ₁ , % predicted	79.0 (71.0–86.0)	79.0 (72.8–85.3)	79.5 (70.0–87.5)	0.987
DL _{CO} , % predicted	46.8 (39.3–61.2)	47.3 (38.3–63.0)	46.5 (40.4–57.7)	0.483
Blood count values				
WBC (×10 ⁹ /L)	6.90 (5.99–8.38)	6.75 (5.92–8.23)	7.61 (6.04–9.41)	0.307
Platelet (×10 ⁹ /L)	243.0 (204.5–281.8)	231.0 (209.3–275.0)	249.7 (199.0–305.5)	0.294
NLR	1.90 (1.29–2.46)	1.67 (1.16–2.23)	2.26 (1.96–3.20)	< 0.001
PLR	106.10 (87.24–140.22)	96.42 (84.73–128.15)	121.03 (96.86–188.49)	0.003
LMR	4.00 (2.98–5.32)	4.33 (3.08–5.72)	3.71 (2.88–4.36)	0.119
SIRI	1.01 (0.66–1.42)	0.91 (0.58–1.31)	1.24 (0.91–1.64)	0.011
AISI	236.81 (142.65–378.37)	215.58 (129.15–336.89)	303.95 (204.21–459.66)	0.024
^b Blood chemistry tests				
Total protein, g/L	74.0 (71.0–78.0); n = 92	74.5 (72.0–78.0); n = 58	73.0 (69.0–78.0); n = 34	0.499
Total cholesterol, mmol/L	5.35 (4.70–6.00); n = 66	5.50 (4.83–6.19); n = 43	5.20 (4.39–5.80); n = 23	0.174
Creatinine, μmol/l	78.5 (66.4–87.0); n = 92	78.9 (66.5–87.0); n = 58	77.7 (65.8–87.0); n = 34	0.596
C-reactive protein, mg/L	4.00 (2.20–7.28); n = 95	3.19 (1.83–6.00); n = 59	6.48 (2.73–11.54); n = 36	0.006
Uric acid, μmol/L	0.37 (0.28–0.42); n = 45	0.38 (0.30–0.45); n = 28	0.35 (0.26–0.42); n = 17	0.440
Lactate dehydrogenase, U/L	216.5 (173.5–297.5); n = 40	208.0 (160.0–323.0); n = 24	231.0 (187.0–284.5); n = 16	0.730
Hemoglobin, g/L	144.0 (133.0–157.0)	147.0 (133.0–157.0)	142.0 (133.2–153.5)	0.362
^c Haemostasis				
Fibrinogen, g/L	3.04 (2.62–3.70); n = 71	2.82 (2.27–3.57); n = 41	3.28 (2.88–4.17); n = 30	0.032
INR	1.08 (0.99–1.20); n = 85	1.10 (1.00–1.22); n = 50	1.05 (0.98–1.16); n = 35	0.179
TCT, seconds	13.00 (12.43–14.05); n = 81	13.00 (12.53–13.98); n = 47	13.10 (12.00–14.50); n = 34	0.629
D-dimer, ng/mL	166.0 (102.0–245.3); n = 44	139.0 (77.5–198.0); n = 25	225.0 (107.0–337.0); n = 19	0.040

Table 1. Demographics and clinical characteristics of study groups. Data are presented as n, n (%) or median (interquartile range). *BMI* body mass index, *FVC* forced vital capacity, *FEV₁* forced expiratory volume in the first second, *DL_{CO}* diffusing capacity of the lung for carbon monoxide, *WBC* white blood cell. *NLR* neutrophil-to-lymphocyte ratio, *PLR* platelet-to-lymphocyte ratio, *LMR* lymphocyte-to-monocyte ratio, *SIRI* systemic inflammatory response index, *AISI* aggregate index of systemic inflammation, *PF-ILD* progressive fibrosing phenotype of interstitial lung disease, *non-PF-ILD* non-progressive fibrosing phenotype of interstitial lung disease, *INR* International normalized ratio, *TCT* thrombin clotting time. ^aSmoking history denotes subjects with > 10 pack-years of cigarette smoking. ^bBlood chemistry tests and ^chaemostasis parameters were analyzed where available. Significant values are in bold.

blood count tests, blood chemistry tests and haemostasis parameters only PLR was positively correlated with mean annual concentration of NO₂ ($R = 0.245$, $p = 0.015$).

Association between biomarker expression and clinical features of subjects with ILDs

The numbers of DP-desq ($R = -0.480$, $p < 0.001$), DP-aw ($R = -0.313$, $p < 0.001$), as well as the levels of CXCL13 ($R = -0.303$, $p = 0.001$), CD206 ($R = -0.244$, $p = 0.011$), and IL-1 β ($R = -0.302$, $p = 0.001$) in the lungs of ILD patients at the study entry were correlated with diffusing capacity of the lung for carbon monoxide (DL_{CO}, % predicted). CD206 at baseline was similarly correlated, albeit even more weakly, with FVC of the subjects with ILDs ($R = -0.192$, $p = 0.046$). Intrapulmonary CXCL13 level was increased in smoking patients with ILDs compared with non-smoking ILD patients. Follow-up analysis of CXCL13 expression depending on both smoking and PM₁₀ concentration showed that CXCL13 level was higher in both smoking and non-smoking patients exposed for ≥ 15 days to polluted air (daily average PM₁₀ concentration of $> 50 \mu\text{g}/\text{m}^3$) compared with patients exposed for < 15 days to the same daily average PM₁₀ concentration (Fig. 6). There were no statistically significant differences in the amount of DP-aw, DP-desq and expression of other biomarkers (IL-1 β , TGF- β 1, TNF α , CTGF, FGF-2, and CD206) in lung tissue samples between smoking patients (current smokers or ex-smokers) with ILDs and non-smoking patients with ILDs. Moreover, the number of DP and biomarker expression in the lungs were not associated with pack-years of smoking (in ever-smokers), sex, age, body mass

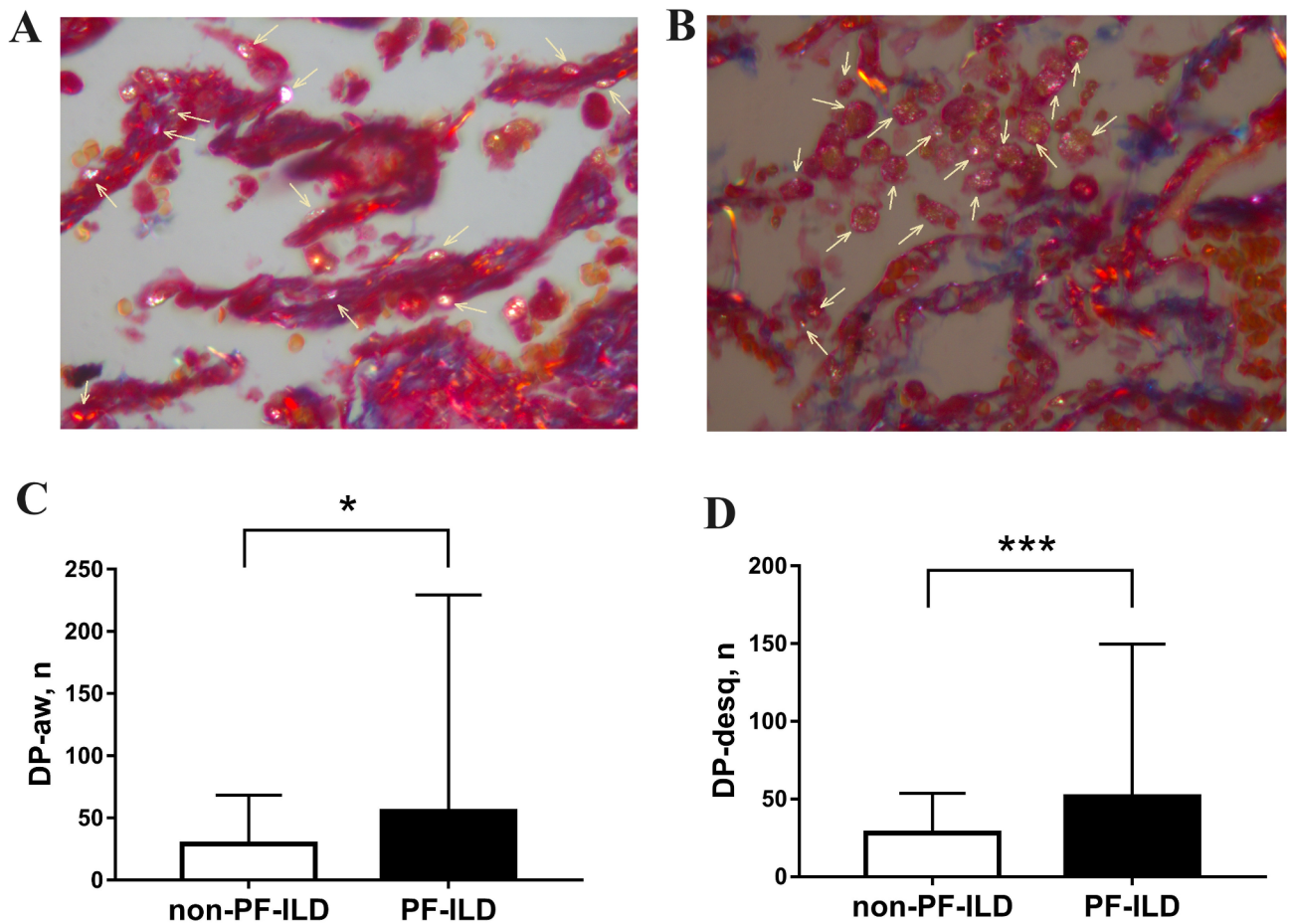


Fig. 2. Dust particles in lung tissue samples from patients with interstitial lung disease (ILD). Yellow arrows point to birefringent dust particles (DP) visualized in polarizing light microscopy at 400 \times magnification in the alveolar wall cells (DP-aw, **A**) and in the desquamated epithelial cells within alveolar spaces (DP-desq, **B**). The numbers of DP-aw (**C**) and DP-desq (**D**) were counted in lung tissue samples from patients with progressive fibrosing (PF-ILD) and non-progressive fibrosing phenotype (non-PF-ILD). Results are expressed as median with interquartile range. * $p < 0.05$; *** $p < 0.001$.

index, occupational history, oxygen saturation, forced expiratory volume in the first second (FEV₁), type of ILD (by aetiology), treatment used at baseline, or death.

Diagnostic accuracy of PF-ILD biomarkers

To evaluate the diagnostic accuracy of the identified biomarkers of PF-ILD, we first performed the univariate logistic regression analysis. Higher blood NLR and PLR values, intrapulmonary CXCL13, IL-1 β , CTGF, TGF- β 1, and CD206 levels, numbers of DP-desq and DP-aw in lung tissue were independent predictors of PF-ILD (Table 2). Blood SIRI and AISI values were not predictive of PF-ILD.

Secondly, we randomly divided all patients into derivation ($n = 80$) and validation ($n = 29$) cohorts (Supplementary Table 1), and performed ROC curve analysis for selected variables in the derivation cohort. Blood NLR and PLR values, intrapulmonary expression of CXCL13, IL-1 β , CTGF, TGF- β 1, and CD206, amount of DP-desq and DP-aw in the lungs were useful in predicting PF-ILD with a sensitivity of 46.2–92.3%, specificity of 55.6–85.2%, and AUC of 0.636–0.745 (Table 3). Among the 9 biomarkers assessed, NLR had the highest AUC (0.745) followed by DP-desq (0.727), IL-1 β (0.716), DP-aw (0.677), TGF- β 1 (0.676), CD206 (0.672), CTGF (0.668), PLR (0.649) and CXCL13 (0.636) levels. Figure 7 shows ROC curves for these biomarkers.

Next, we investigated the predictive value of different biomarker combinations. Combining three markers increased predictive accuracy, with the best AUC of 0.847, sensitivity of 84.6%, specificity of 83.3%, positive predictive value (PPV) of 75.9%, and negative predictive value (NPV) of 91.9%, obtained using a combination of NLR, CD206, and DP-desq. Supplementary material section shows the prognostic model equation 1. The multivariate logistic analysis suggested that NLR, CD206 and DP-desq are independent risk factors for predicting PF-ILD (Table 4). Youden index J for this model was 0.680, the Hosmer-Lemeshow χ^2 value was 12.174 ($p = 0.144$), Cox & Snell R^2 was 0.284, and Nagelkerke R^2 was 0.396. Testing the model in the validation cohort of patients confirmed its high predictive accuracy with a sensitivity of 80.0%, specificity of 84.2%, PPV of 72.7%, and NPV of 88.9%.

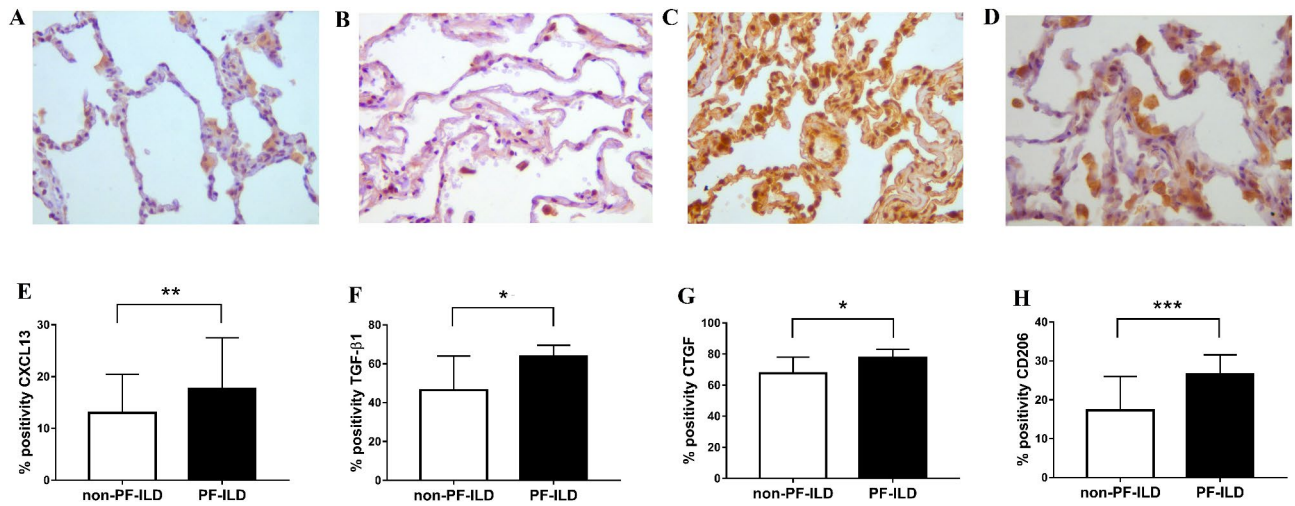


Fig. 3. Intrapulmonary M2 macrophage marker expression in interstitial lung disease (ILD) patients. Positive immunoreactivity to (A) CXCL13, (B) transforming growth factor β 1 (TGF- β 1), (C) connective tissue growth factor (CTGF), and (D) CD206 was visualized by immunohistochemistry and 3,3'-diaminobenzidine (DAB) detection chromogen (brown). Sections were counterstained with Mayer's hematoxylin (blue). All images were taken at 400 \times magnification. Positivity (%) of (E) CXCL13, (F) TGF- β 1, (G) CTGF, and (H) CD206 pulmonary expression was compared between ILD patients with progressive fibrosis (PF-ILD) and non-progressive fibrosis phenotype (non-PF-ILD). Results are expressed as median with interquartile range. * $p < 0.05$; ** $p < 0.01$; *** $p < 0.001$.

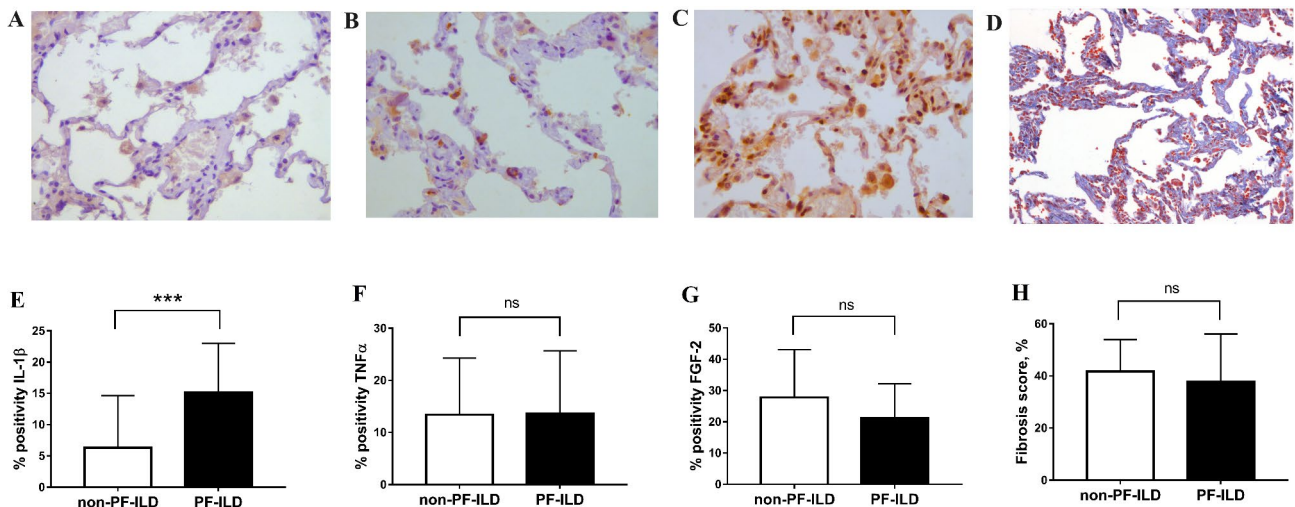


Fig. 4. Intrapulmonary M1 and M2 macrophage marker expression and fibrosis score in interstitial lung disease (ILD) patients. Immunostaining of (A) interleukin 1 β (IL-1 β), (B) tumor necrosis factor α (TNF α), and (C) fibroblast growth factor 2 (FGF-2) in lung tissue specimens was observed by immunohistochemistry and 3,3'-diaminobenzidine (DAB) detection chromogen (brown). Sections were counterstained with Mayer's hematoxylin (blue). Masson's trichrome staining of lung tissues (D) was used to calculate fibrosis score. Images (A–C) were taken at 400 \times magnification, while image (D) was taken at 200 \times magnification. Expression of (E) IL-1 β , (F) TNF α , (G) FGF-2, and (H) fibrosis score were compared between ILD patients with progressive fibrosis (PF-ILD) and non-progressive fibrosis phenotype (non-PF-ILD). Results are expressed as median with interquartile range. *** $p < 0.001$; ns not significant.

Discussion

In this investigation, we revealed new approaches for the prognosis of PF-ILD other than IPF. A progressive phenotype was identified in approximately one-third of patients with fibrosing ILDs, and was associated with high positivity of CD206, CXCL13, IL-1 β , TGF- β 1, and CTGF expression, as well as increased numbers of DP-aw and DP-desq in lung tissue samples. Some of these biomarkers (CXCL13, IL-1 β and CD206 expression, the number of DP-desq in the lungs) were higher in patients who lived for ≥ 15 days in the areas with 24-

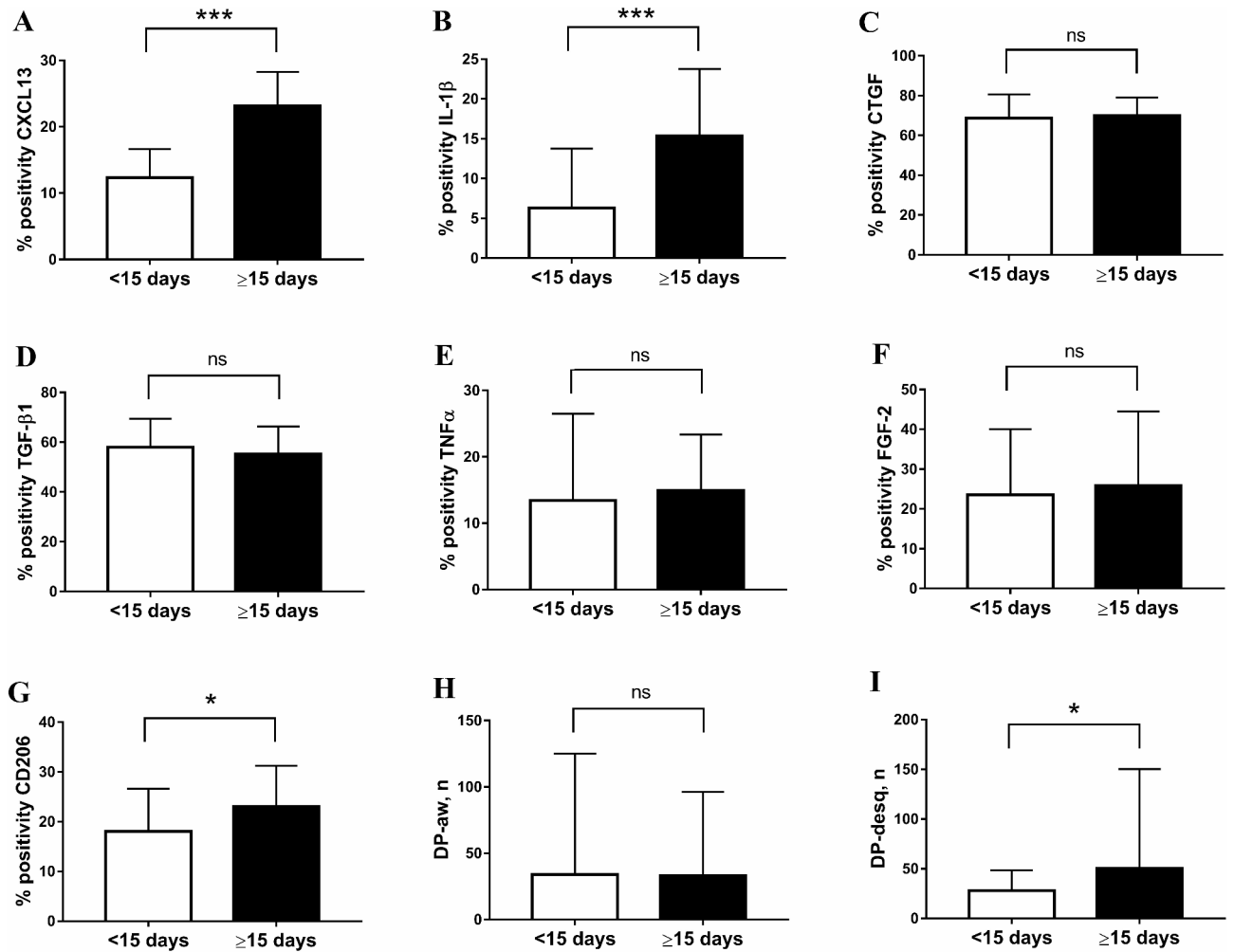


Fig. 5. The effect of high daily average PM_{10} concentration on the pulmonary expression of M1/M2 macrophage markers and the amount of dust particles (DP) in the lungs of patients with interstitial lung disease. Intrapulmonary expression of (A) CXCL13, (B) interleukin 1 β (IL-1 β), (C) tumor necrosis factor α (TNF α), (D) fibroblast growth factor 2 (FGF-2), (E) transforming growth factor β 1 (TGF- β 1), (F) connective tissue growth factor (CTGF), (G) CD206, and the numbers of (H) DP-aw (dust particles in the alveolar wall cells), (I) DP-desq (dust particles in the desquamated epithelial cells) were compared between ILD patients who lived for ≥ 15 days ($n = 57$) and ILD patients who resided for < 15 days ($n = 40$) in places with daily ambient PM_{10} level of more than $50 \mu\text{g}/\text{m}^3$. Results are expressed as median with interquartile range. * $p < 0.05$; *** $p < 0.001$; ns not significant.

hour ambient PM_{10} level of more than $50 \mu\text{g}/\text{m}^3$ compared with patients exposed for fewer days to the similar PM_{10} concentration. Our study also demonstrated the efficacy of blood tests (NLR and PLR) in predicting PF-ILD. Finally, using logistic regression analysis, we developed a model consisting of 3 biomarkers (CD206 level, number of DP-desq in lung tissue, and NLR), which demonstrated promising potential for predicting PF-ILD with an AUC of 0.847, sensitivity of 84.6%, and specificity of 83.3%.

Risk factors for progression of fibrosing ILDs are currently being extensively studied. In the numerous studies, smoking, endothelial dysfunction, and lung infection have been demonstrated to trigger fibrotic changes in the lungs³⁰. We have previously shown that metal oxide nanoparticles (MeONPs) in the mouse lungs possess fibrogenic potential. Inhalation exposure to MeONPs leads to their accumulation in the lungs and subsequently induce pulmonary inflammation³¹. In this work, using polarizing light microscopy, we calculated the number of DP in lung tissue sections from patients with ILDs. DP were found in all samples, with the highest count reaching a maximum of 1085 particles per sample (in 10 random fields of view). Although we did not determine elemental composition of DP, a previous study using energy dispersive spectrometry with a field emission scanning electron microscope has identified elements such as silicon, aluminum, potassium, iron, calcium, sodium, magnesium, sulfur, chromium, and copper in the particles from lung tissue samples of IPF patients¹³. In addition, it is well established that crystalline silica (SiO_2), aluminum and its oxides cause pulmonary fibrosis in patients with pneumoconiosis^{32,33}. In our study, the numbers of DP-desq and DP-aw were higher in PF-ILD patients compared with non-PF-ILD patients, suggesting a possible role of DP in the progression of pulmonary

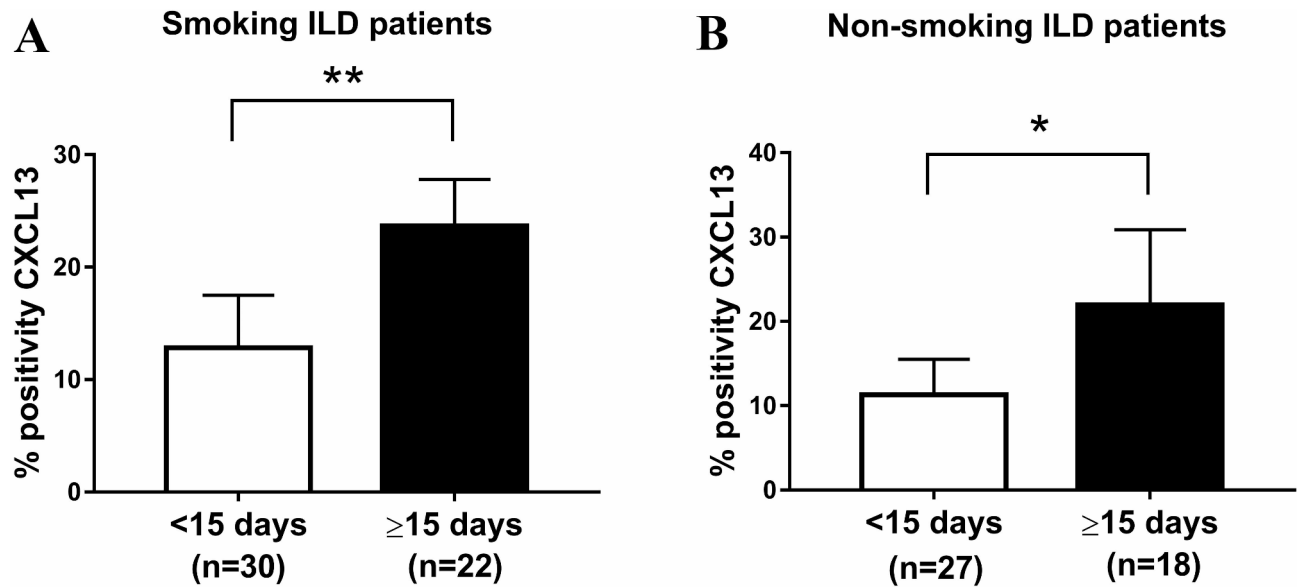


Fig. 6. Effect of both smoking and PM_{10} exposure on the intrapulmonary CXCL13 level. CXCL13 expression in lung tissues from (A) smoking and (B) non-smoking patients with ILDs is shown in subjects exposed for ≥ 15 days to 24-hour average PM_{10} concentration of $> 50 \mu\text{g}/\text{m}^3$ (≥ 15 days) in comparison with patients exposed for < 15 days to PM_{10} with daily average concentration of $> 50 \mu\text{g}/\text{m}^3$ (< 15 days). Results are expressed as median with interquartile range. * $p < 0.05$; ** $p < 0.01$.

Biomarker	Unadjusted ($n = 109$)		Adjusted* ($n = 97$)	
	OR (95% CI)	<i>p</i> -value	OR (95% CI)	<i>p</i> -value
NLR	1.873 (1.248–2.811)	0.002	2.552 (1.468–4.437)	<0.001
PLR	1.010 (1.003–1.017)	0.008	1.012 (1.003–1.020)	0.006
SIRI	1.115 (0.812–1.531)	0.500	1.455 (0.812–2.608)	0.208
AISI	1.001 (0.999–1.002)	0.344	1.001 (0.999–1.003)	0.190
CXCL13	1.056 (1.012–1.102)	0.013	1.059 (1.003–1.118)	0.039
IL-1 β	1.068 (1.025–1.113)	0.002	1.078 (1.024–1.135)	0.004
CTGF	1.040 (1.002–1.079)	0.040	1.049 (1.003–1.096)	0.036
TGF- β 1	1.028 (1.005–1.051)	0.016	1.041 (1.012–1.071)	0.005
CD206	1.085 (1.032–1.141)	0.001	1.094 (1.026–1.166)	0.006
DP-desq, n	1.005 (1.001–1.009)	0.009	1.005 (1.001–1.010)	0.032
DP-aw, n	1.004 (1.001–1.008)	0.014	1.004 (1.000–1.009)	0.039

Table 2. Univariate odds ratios (unadjusted and adjusted) for predictive markers of progressive fibrosing interstitial lung disease (PF-ILD). ORs (odds ratios) are presented per unit change in log₂-transformed biomarker level. *Adjusted logistic models for 65 non-PF-ILD patients and 32 PF-ILD patients with available data on air pollution exposure were adjusted by age, gender, smoking status, baseline FVC % predicted, DL_{CO} % predicted, annual mean levels of PM_{10} and NO_2 . NLR neutrophil-to-lymphocyte ratio, PLR platelet-to-lymphocyte ratio, SIRI systemic inflammatory response index, AISI aggregate index of systemic inflammation, TGF- β 1 transforming growth factor β 1, CTGF connective tissue growth factor, IL-1 β interleukin 1 β , DP-desq dust particles in the desquamated epithelial cells within the alveolar spaces, DP-aw dust particles in the alveolar wall cells. Significant values are in bold.

fibrosis. Interestingly, there was no association between the number of DP and pack-years of smoking in ever-smoking patients with ILD. In addition, the amount of DP was similar in lung tissue samples from smoking and non-smoking patients with ILDs. Mäkelä and colleagues¹³ found inverse correlation of DP scores in the lungs and pack-years of smoking in IPF patients, indicating no stimulating effect of smoking on the numbers of DP in the lungs.

More importantly, we observed that the number of DP-desq was higher in ILD patients from regions, where the daily average PM_{10} concentration exceeded $50 \mu\text{g}/\text{m}^3$ for 15 or more days per year, compared with those exposed for less than 15 days per year to the similar PM_{10} concentration. This finding highlights the contribution of air pollution to the mechanisms of lung injury in ILDs. It is worth noting that 2021 WHO global air quality

Biomarker	AUC	Cut-off	Sensitivity	Specificity	PPV	NPV
NLR	0.745	>1.80	92.3%	55.6%	50.0%	93.8%
PLR	0.649	>140	46.2%	81.5%	54.5%	75.9%
CXCL13, %	0.636	>15.33	73.1%	63.0%	48.7%	82.9%
IL-1 β , %	0.716	>13.33	69.2%	70.4%	52.9%	82.6%
CTGF, %	0.668	>69.4	73.1%	64.8%	50.0%	83.3%
TGF- β 1, %	0.676	>49.4	76.9%	59.3%	47.6%	84.2%
CD206, %	0.672	>29	46.2%	85.2%	60.0%	76.7%
DP-desq, n	0.727	>50	57.7%	77.8%	55.6%	79.2%
DP-aw, n	0.677	>43	61.5%	72.2%	51.6%	79.6%

Table 3. Area under the curve (AUC), cut-off value, sensitivity, specificity, positive predictive value (PPV), and negative predictive value (NPV) for the prediction of progressive fibrosing interstitial lung disease by each biomarker. *NLR* neutrophil-to-lymphocyte ratio, *PLR* platelet-to-lymphocyte ratio, *IL-1 β* interleukin 1 β , *CTGF* connective tissue growth factor, *TGF- β 1* transforming growth factor β 1, *DP-desq* dust particles in the desquamated epithelial cells within the alveolar spaces, *DP-aw* dust particles in the alveolar wall cells.

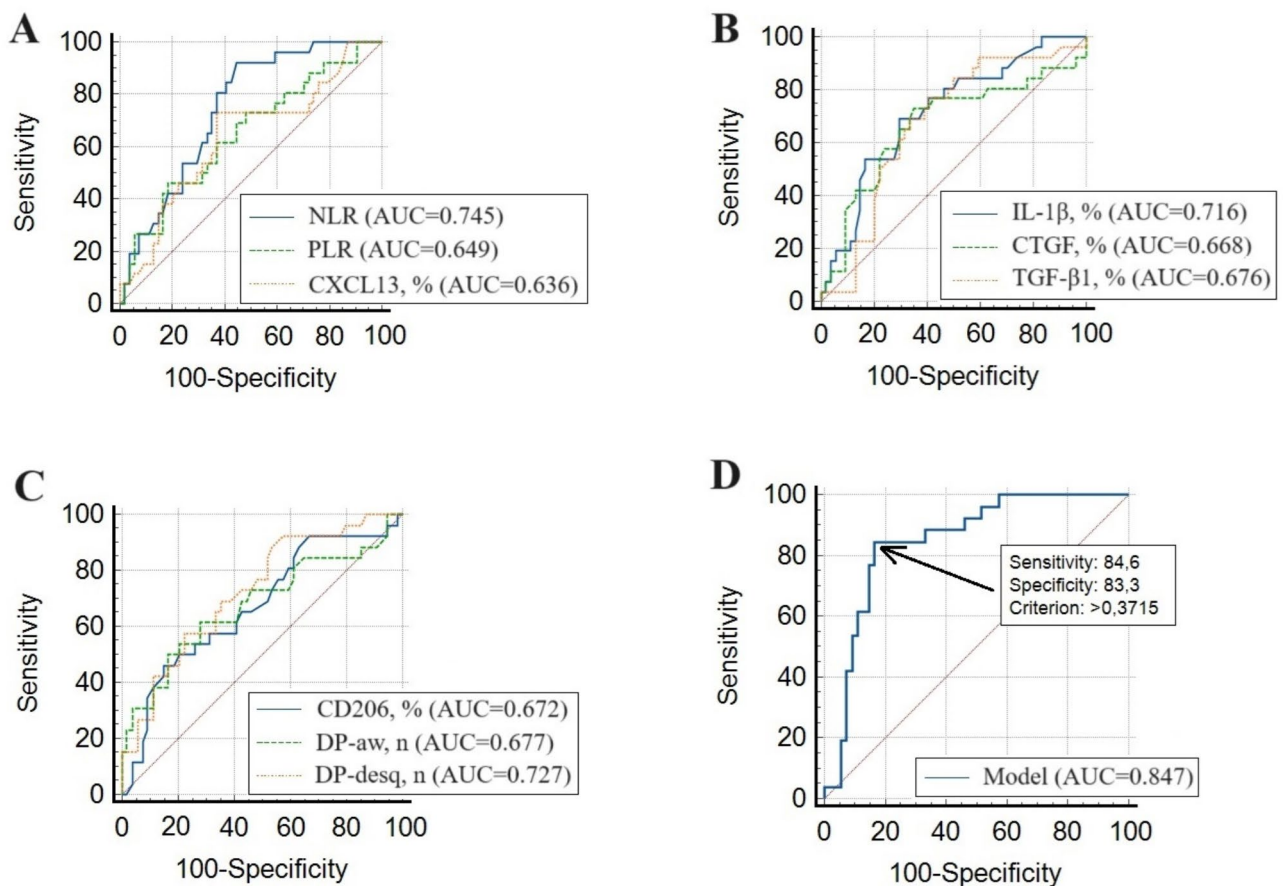


Fig. 7. Area under the receiver operating characteristics curve (AUROC) of the biomarkers to predict progressive fibrosing interstitial lung disease. (A) NLR (neutrophil-to-lymphocyte ratio), PLR (platelet-to-lymphocyte ratio), CXCL13 (%); (B) CTGF (connective tissue growth factor, %), IL-1 β (interleukin 1 β), TGF- β 1 (transforming growth factor β 1, %); (C) CD206 (%), DP-desq (dust particles in the desquamated epithelial cells, n), DP-aw (dust particles in the alveolar wall cells, n); (D) combined model constructed as a result of the regression equation.

guidelines (AQGs) recommend setting the 24-hour average level for PM₁₀ at 45 $\mu\text{g}/\text{m}^3$, and introduced an interim target 4 (50 $\mu\text{g}/\text{m}^3$) at the level of the 2005 AQGs³⁴. In the current study, we assessed the effect of air pollution on DP numbers and biomarkers in the lung biopsy specimens of patients who underwent VATS procedure between January 1, 2015 and December 31, 2021, when 2005 AQGs were mainly in force. Greater numbers of DP

Biomarker	Odds ratio (95% CI)	<i>p</i> -value
NLR	2.330 (1.373–3.953)	0.002
CD206, %	1.121 (1.042–1.206)	0.002
DP-desq, n	1.007 (1.002–1.012)	0.007

Table 4. Best logistic regression model for the prediction of progressive fibrosing interstitial lung disease based on 3 biomarkers. *NLR* neutrophil-to-lymphocyte ratio, *DP-desq* dust particles in the desquamated epithelial cells within the alveolar spaces. Significant values are in bold.

and more severe fibrotic alterations in the lungs were also found in patients, residents of Mexico City, Mexico, exposed to high levels of ambient PM compared with patients living in Vancouver, British Columbia, Canada, a region with low PM levels³⁵.

We further observed that patients with large numbers of DP-desq (≥ 50 in 10 random fields of view per sample) in lung tissue had higher expression of CXCL13, IL-1 β , and CD206 compared with patients with small amount (< 50) of DP-desq. These findings suggest that DP can stimulate production of CXCL13, IL-1 β , and CD206. We speculate that this can be a result of macrophage differentiation into M2 type induced by DP (Supplementary Fig. 2). Phenotypically M2 macrophages are characterized by the expression of a wide range of proteins, including TGF- β 1, CTGF, CXCL13, FGF-2, and CD206, while TNF α and IL-1 β are overlapping cytokines secreted by both M1 and M2 macrophages^{20,21,36}.

The macrophage mannose receptor (CD206) is a transmembrane glycoprotein expressed by M2 alternatively activated macrophages³⁷. CD206+ M2 macrophages promote myofibroblast differentiation³⁸, activate resident fibroblasts through the release of TGF- β 1, platelet-derived growth factor (PDGF), vascular endothelial growth factor (VEGF), insulin-like growth factor 1 (IGF-1), galactin-3³⁹, and can differentiate into fibrocyte-like cells that express collagen⁴⁰, aggravating the progression of pulmonary fibrosis. In a murine model of bleomycin-induced pulmonary fibrosis, targeting the CD206 receptor in M2-like macrophages with synthetic peptide RP-832c reduced extent of fibrosis and inhibited production of TGF- β 1, matrix metalloproteinase 13 (MMP-13), IL-6, IL-10, TNF α , interferon γ , and CXCL1/2 in the lungs⁴¹. In this study, we have revealed CD206 as a new biomarker of PF-ILD with an AUC of 0.672, sensitivity of 46.2%, and specificity of 85.2%.

Recent studies showed that besides follicular dendritic cells and B-lymphocytes, CXCL13 is also secreted by M2 macrophages^{42,43}. In particular, CXCL13 was found in CD206+ alveolar macrophages from patients with IPF⁴³. CXCL13 through the cognate receptor CXCR5 is involved in the recruitment of B cells and follicular helper T cells towards B cell follicles in secondary lymphoid organs⁴⁴. Blood CXCL13 concentration was associated with IPF severity and progression⁴⁵. Our study provides a previously undocumented elevation of CXCL13 expression in lung tissue of PF-ILD patients caused by both smoking and PM₁₀ exposure. Broadly comparable findings on the effects of smoking and air pollution have been reported in non-small cell lung cancers (NSCLCs) studies, in which increased CXCL13 expression in tumor samples was associated with smoking and living in Xuanwei City of Yunnan Province, China, a highly polluted region⁴⁶.

Within this study, IL-1 β expression in lung tissue was found to be elevated in patients with PF-ILD compared with non-PF-ILD patients and it was inversely correlated with DL_{CO}. At a cut-off value of 13.33%, the sensitivity and specificity of IL-1 β in predicting PF-ILD were 69.2% and 70.4%, respectively, with an AUC of 0.716. The results suggest that IL-1 β is useful as a prognostic biomarker for progressive fibrosing phenotype in patients with ILD. M. Kolb et al. previously described the mechanism underlying IL-1 β action in pulmonary fibrosis. Overexpression of IL-1 β in rats induced an increase of pulmonary myofibroblasts and deposition of collagen in the interstitium, leading to severe and progressive pulmonary fibrosis⁴⁷. Our findings demonstrate that IL-1 β level was higher in patients resided for ≥ 15 days in places with 24-hour ambient PM₁₀ level of more than 50 $\mu\text{g}/\text{m}^3$, suggesting an effect of air pollution on IL-1 β expression in lung tissue. Taking into account greater expression of IL-1 β in patients with large numbers of DP-desq in lung tissue, we assume that IL-1 β level is affected by air pollution through DP, i.e. primarily, DP are accumulated in lung tissue of PF-ILD patients in response to PM₁₀ inhalation, and subsequently stimulate the expression of IL-1 β . In agreement with our findings, exposure to silica crystal, widely present in DP, activated IL-1 β in human immune cells and induced influx of neutrophils into the lung through IL-1 β ⁴⁸.

An accurate prognosis of PF-ILD is critical as initiating inappropriate treatment increase risk of adverse events and treatment failure⁷. This has been previously addressed in a number of studies aimed at finding predictors of PF-ILD among biological, clinical, functional, and radiological variables. Clubbing of fingers and HRCT-documented usual interstitial pneumonia (UIP)-like fibrotic pattern were risk factors for fibrosis progression in a cohort of patients, including both IPF and non-IPF-ILD patients (IPF/non-IPF-ILD)⁴⁹. Cellular analysis of the bronchoalveolar lavage fluid identified neutrophils, lymphocytes, CD8 T cells, and NLR as independent predictive markers of progressive fibrosing phenotype in IPF/non-IPF-ILD patients with an AUC of 0.59–0.66, sensitivity of 57–77% and specificity of 53–70%⁵⁰. A meta-analysis of NLR in ILD revealed that increased NLR levels predicted poor outcomes in IPF/non-IPF-ILD patients⁵¹. In the current study, we found biomarkers of non-IPF PF-ILD, paying particular attention to the exclusion of patients with IPF from the study. Compared with single biomarker, the combination of CD206 expression, number of DP-desq in lung tissue and blood NLR value showed better accuracy for predicting PF-ILD (AUC=0.847), with a higher sensitivity of 84.6%, and specificity of 83.3%. Importantly, high predictive accuracy of the proposed model was confirmed in the validation cohort of ILD patients. The approach based on the combination of several biomarkers to improve the accuracy of prognosis was previously demonstrated in IPF studies. In particular, the combination of ficolin-2,

cathepsin-S, legumain, soluble vascular endothelial growth factor receptor 2, inducible T cell costimulator, and trypsin 3 levels better predicted progression-free survival in IPF patients than each single analyte⁵². Combination of the progression index with the GAP (gender, age and physiology) score significantly improved the capacity to distinguish IPF progression at 12 months above GAP alone⁵³.

Our results should be interpreted within the limitations of the study. First, this was a retrospective single-center study, indicating a potential risk of selection bias. Second, there are only two air pollution stations in the Republic of Belarus, which measure PM_{2.5}. As a result, it was impossible to search for associations between biomarkers in lung tissue and the level of ambient PM_{2.5}. Although, given the size of PM_{2.5}, one would have expected an even closer association of the number of DP in the lungs with ambient air concentration of PM_{2.5}, than exposure to PM₁₀. Third, blood chemistry tests and haemostasis parameters were missing in some patients, which did not allow to assess the diagnostic accuracy for using CRP, fibrinogen and D-dimer concentration in the peripheral blood to predict progression of fibrosing ILDs.

Conclusions

In conclusion, the present study demonstrated the diagnostic value of DP-desq, DP-aw, CD206, CXCL13, IL-1 β , TGF- β 1, and CTGF expression in lung tissue, as well as blood NLR and PLR values for PF-ILD prediction. The combination of CD206 expression, number of DP-desq, and blood NLR significantly enhanced diagnostic performance of PF-ILD biomarkers. Furthermore, we found the association of the number of DP-desq, pulmonary expression of CXCL13, IL-1 β and CD206 with residence in places characterized by high daily average PM₁₀ concentration, highlighting the need for reducing pollutant emission.

Data availability

The datasets generated and/or analysed during the current study are not publicly available but are available from the corresponding author upon reasonable request.

Received: 26 November 2024; Accepted: 5 March 2025

Published online: 20 March 2025

References

- Martinez, F. J. et al. Idiopathic pulmonary fibrosis. *Nat. Rev. Dis. Primers* **3**, 17074 (2017).
- Alsomali, H., Palmer, E., Aujayeb, A. & Funston, W. Early diagnosis and treatment of idiopathic pulmonary fibrosis: a narrative review. *Pulm. Ther.* **9** (2), 177–193 (2023).
- Torrisi, S. E. et al. Outcomes and incidence of PF-ILD according to different definitions in a real-world setting. *Front. Pharmacol.* **12**, 790204 (2021).
- Raghu, G. et al. Idiopathic pulmonary fibrosis (an update) and progressive pulmonary fibrosis in adults: an official ATS/ERS/JRS/ALAT clinical practice guideline. *Am. J. Respir. Crit. Care Med.* **205** (9), e18–e47 (2022).
- Komatsu, M. et al. Clinical characteristics of non-idiopathic pulmonary fibrosis, progressive fibrosing interstitial lung diseases: A single-center retrospective study. *Medicine (Baltim)*. **100** (13), e25322 (2021).
- Brown, K. K. et al. The natural history of progressive fibrosing interstitial lung diseases. *Eur. Respir. J.* **55** (6), 2000085 (2020).
- Rajan, S. K. et al. Progressive pulmonary fibrosis: an expert group consensus statement. *Eur. Respir. J.* **61** (3), 2103187 (2023).
- Kapnadak, S. G. & Raghu, G. Lung transplantation for interstitial lung disease. *Eur. Respir. Rev.* **30** (161), 210017 (2021).
- Inoue, Y. et al. Diagnostic and prognostic biomarkers for chronic fibrosing interstitial lung diseases with a progressive phenotype. *Chest* **158** (2), 646–659 (2020).
- Majewski, S. & Piotrowski, W. J. Air pollution—an overlooked risk factor for idiopathic pulmonary fibrosis. *J. Clin. Med.* **10** (1), 77 (2020).
- Mariscal-Aguilar, P. et al. Air pollution exposure and its effects on idiopathic pulmonary fibrosis: clinical worsening, lung function decline, and radiological deterioration. *Front. Public Health* **11**, 1331134 (2024).
- Kayalar, Ö. et al. Impact of particulate air pollution on airway injury and epithelial plasticity; underlying mechanisms. *Front. Immunol.* **15**, 1324552 (2024).
- Mäkelä, K. et al. Inorganic particulate matter in the lung tissue of idiopathic pulmonary fibrosis patients reflects population density and fine particle levels. *Ann. Diagn. Pathol.* **40**, 136–142 (2019).
- Rabeyrin, M. et al. Usual interstitial pneumonia end-stage features from explants with radiologic and pathological correlations. *Ann. Diagn. Pathol.* **19** (4), 269–276 (2015).
- Tsuchiya, K. et al. Elemental analysis of inorganic dusts in lung tissues of interstitial pneumonias. *J. Med. Dent. Sci.* **54** (1), 9–16 (2007).
- Nasr, M. R. et al. Inorganic dust exposure causes pulmonary fibrosis in smokers: analysis using light microscopy, scanning electron microscopy, and energy dispersive X-ray spectroscopy. *Arch. Environ. Occup. Health* **61** (2), 53–60 (2006).
- Marín-Palma, D. et al. Particulate matter impairs immune system function by up-regulating inflammatory pathways and decreasing pathogen response gene expression. *Sci. Rep.* **13** (1), 12773 (2023).
- Valderrama, A. et al. Particulate matter (PM₁₀) induces in vitro activation of human neutrophils, and lung histopathological alterations in a mouse model. *Sci. Rep.* **12** (1), 7581 (2022).
- Li, C. H. et al. Role of macrophages in air pollution exposure related asthma. *Int. J. Mol. Sci.* **23** (20), 12337 (2022).
- Strizova, Z. et al. M1/M2 macrophages and their overlaps—myth or reality? *Clin. Sci.* **137** (15), 1067–1093 (2023).
- Shen, L., Li, Y. & Zhao, H. Fibroblast growth factor signaling in macrophage polarization: impact on health and diseases. *Front. Immunol.* **15**, 1390453 (2024).
- Mikolasch, T. A. et al. Multi-center evaluation of baseline neutrophil-to-lymphocyte (NLR) ratio as an independent predictor of mortality and clinical risk stratifier in idiopathic pulmonary fibrosis. *EClinicalMedicine* **55**, 101758 (2022).
- Stock, C. J. W. et al. Serum C-reactive protein is associated with earlier mortality across different interstitial lung diseases. *Respirology* **29** (3), 228–234 (2024).
- Zinellu, A. et al. Blood cell count derived inflammation indexes in patients with idiopathic pulmonary fibrosis. *Lung* **198** (5), 821–827 (2020).
- Flaherty, K. R. et al. Nintedanib in progressive fibrosing interstitial lung diseases. *N. Engl. J. Med.* **381** (18), 1718–1727 (2019).
- Hambly, N. et al. Prevalence and characteristics of progressive fibrosing interstitial lung disease in a prospective registry. *Eur. Respir. J.* **60** (4), 2102571 (2022).

27. Zhou, Q. et al. Intratracheal instillation of high dose adenoviral vectors is sufficient to induce lung injury and fibrosis in mice. *PLoS One* **9** (12), e116142 (2014).
28. Chieosilapatham, P. et al. Comparative immunohistochemical analysis of inflammatory cytokines in distinct subtypes of sweet syndrome. *Front. Immunol.* **15**, 1355681 (2024).
29. Chlipala, E. A. et al. An image analysis solution for quantification and determination of immunohistochemistry staining reproducibility. *Appl. Immunohistochem. Mol. Morphol.* **28** (6), 428–436 (2020).
30. D'Agnano, V. et al. Targeting progression in pulmonary fibrosis: an overview of underlying mechanisms, molecular biomarkers, and therapeutic intervention. *Life* **14** (2), 229 (2024).
31. Cao, J. et al. Deciphering key nano-bio interface descriptors to predict nanoparticle-induced lung fibrosis. *Part. Fibre Toxicol.* **22**, 1 (2025).
32. Honma, K. et al. Proposed criteria for mixed-dust pneumoconiosis: definition, descriptions, and guidelines for pathologic diagnosis and clinical correlation. *Hum. Pathol.* **35** (12), 1515–1523 (2004).
33. Smolkova, P. & Nakladalova, M. The etiology of occupational pulmonary aluminosis—the past and the present. *Biomed. Pap Med. Fac. Univ. Palacky Olomouc Czech Repub.* **158** (4), 535–538 (2014).
34. WHO global air quality guidelines: particulate matter (PM_{2.5} and PM₁₀), ozone, nitrogen dioxide, sulfur dioxide and carbon monoxide. <https://www.who.int/publications/i/item/9789240034228> (2021).
35. Churg, A., Brauer, M., del Carmen Avila-Casado, M., Fortoul, T. I. & Wright, J. L. Chronic exposure to high levels of particulate air pollution and small airway remodeling. *Environ. Health Perspect.* **111** (5), 714–718 (2003).
36. Zhang, S. M. et al. M2-polarized macrophages mediate wound healing by regulating connective tissue growth factor via AKT, ERK1/2, and STAT3 signaling pathways. *Mol. Biol. Rep.* **48** (9), 6443–6456 (2021).
37. Azad, A. K., Rajaram, M. V. & Schlesinger, L. S. Exploitation of the macrophage mannose receptor (CD206) in infectious disease diagnostics and therapeutics. *J. Cytol. Mol. Biol.* **1** (1), 1000003 (2014).
38. Hou, J. et al. M2 macrophages promote myofibroblast differentiation of LR-MSCs and are associated with pulmonary fibrogenesis. *Cell. Commun. Signal.* **16** (1), 89 (2018).
39. Braga, T. T., Agudelo, J. S. & Camara, N. O. Macrophages during the fibrotic process: M2 as friend and foe. *Front. Immunol.* **6**, 602 (2015).
40. Kishore, A. & Petrek, M. Roles of macrophage polarization and macrophage-derived MiRNAs in pulmonary fibrosis. *Front. Immunol.* **12**, 678457 (2021).
41. Ghebremedhin, A. et al. A novel CD206 targeting peptide inhibits bleomycin-induced pulmonary fibrosis in mice. *Cells* **12** (9), 1254 (2023).
42. Xie, Y. et al. M2 macrophages secrete CXCL13 to promote renal cell carcinoma migration, invasion, and EMT. *Cancer Cell. Int.* **21** (1), 677 (2021).
43. Bellamri, N. et al. TNF- α and IL-10 control CXCL13 expression in human macrophages. *J. Immunol.* **204** (9), 2492–2502 (2020).
44. Harrer, C. et al. The CXCL13/CXCR5 immune axis in health and disease-implications for intrathecal B cell activities in neuroinflammation. *Cells* **11** (17), 2649 (2022).
45. Yuga, L. J. et al. C-X-C motif chemokine 13 (CXCL13) is a prognostic biomarker of idiopathic pulmonary fibrosis. *Am. J. Respir. Crit. Care Med.* **189** (8), 966–974 (2014).
46. Wang, G. Z. et al. The chemokine CXCL13 in lung cancers associated with environmental polycyclic aromatic hydrocarbons pollution. *Elife* **4**, e09419 (2015).
47. Kolb, M., Margetts, P. J., Anthony, D. C., Pitossi, F. & Gauldie, J. Transient expression of IL-1 β induces acute lung injury and chronic repair leading to pulmonary fibrosis. *J. Clin. Investig.* **107** (12), 1529–1536 (2001).
48. Hornung, V. et al. Silica crystals and aluminum salts activate the NALP3 inflammasome through phagosomal destabilization. *Nat. Immunol.* **9** (8), 847–856 (2008).
49. Wang, Y. et al. Prognostic predictive characteristics in patients with fibrosing interstitial lung disease: a retrospective cohort study. *Front. Pharmacol.* **13**, 924754 (2022).
50. Watase, M. et al. Diagnostic and prognostic biomarkers for progressive fibrosing interstitial lung disease. *PLoS One* **18** (3), e0283288 (2023).
51. Dong, F., Zheng, L., An, W., Xue, T. & Zhong, X. A meta-analysis of the clinical significance of neutrophil-to-lymphocyte ratios in interstitial lung disease. *PLoS One* **18** (6), e0286956 (2023).
52. Ashley, S. L. et al. Six-SOMAmer index relating to immune, protease and angiogenic functions predicts progression in IPF. *PLoS One* **11** (8), e0159878 (2016).
53. Clynick, B. et al. Biomarker signatures for progressive idiopathic pulmonary fibrosis. *Eur. Respir. J.* **59** (3), 2101181 (2022).

Author contributions

AK designed the study, analyzed the data, and wrote the main manuscript text. OY and NL collected patient data, performed morphological study, immunohistochemical analysis and determined the number of dust particles in the lungs. ED collected patient data. VF and VD were responsible for data analysis and visualization. XC supervised the study. All authors reviewed and edited the manuscript and approved the final version.

Funding

This study was carried out as part of a joint Belarusian-Chinese scientific project (grant from the Belarusian Republican Foundation for Fundamental Research no. M23KITG-002).

Declarations

Ethics approval and consent to participate

The study was approved by the ethics committee of Belarusian State Medical University (Protocol no. 1, August 31, 2023). All procedures were performed in accordance with the principles of the Declaration of Helsinki. Considering the retrospective design, compliance of the study protocol with relevant guidelines and regulations and due to the anonymization of patient data, the informed consent requirement was waived by the ethics committee of Belarusian State Medical University.

Competing interests

The authors declare no competing interests.

Additional information

Supplementary Information The online version contains supplementary material available at <https://doi.org/10.1038/s41598-025-93221-z>.

Correspondence and requests for materials should be addressed to A.K.

Reprints and permissions information is available at www.nature.com/reprints.

Publisher's note Springer Nature remains neutral with regard to jurisdictional claims in published maps and institutional affiliations.

Open Access This article is licensed under a Creative Commons Attribution-NonCommercial-NoDerivatives 4.0 International License, which permits any non-commercial use, sharing, distribution and reproduction in any medium or format, as long as you give appropriate credit to the original author(s) and the source, provide a link to the Creative Commons licence, and indicate if you modified the licensed material. You do not have permission under this licence to share adapted material derived from this article or parts of it. The images or other third party material in this article are included in the article's Creative Commons licence, unless indicated otherwise in a credit line to the material. If material is not included in the article's Creative Commons licence and your intended use is not permitted by statutory regulation or exceeds the permitted use, you will need to obtain permission directly from the copyright holder. To view a copy of this licence, visit <http://creativecommons.org/licenses/by-nc-nd/4.0/>.

© The Author(s) 2025